# Supporting Information

## Catalytic transfer hydrogenation of bio-based furfural with NiO nanoparticles

Jian He,[a,b] Leonhard Schill,[b] Song Yang,[a,*] Anders Riisager[b,*]

[a] *State Key Laboratory Breeding Base of Green Pesticide & Agricultural Bioengineering, Key Laboratory of Green Pesticide & Agricultural Bioengineering, Ministry of Education, State-Local Joint Laboratory for Comprehensive Utilization of Biomass, Center for Research & Development of Fine Chemicals, Guizhou University, Guiyang 550025, PR China.*

[b] *Centre for Catalysis and Sustainable Chemistry, Department of Chemistry, Kemitorvet Building 207, Technical University of Denmark, DK-2800 Kgs. Lyngby, Denmark.*

**(Summary of Content: 16 pages, 3 tables and 9 figures)**

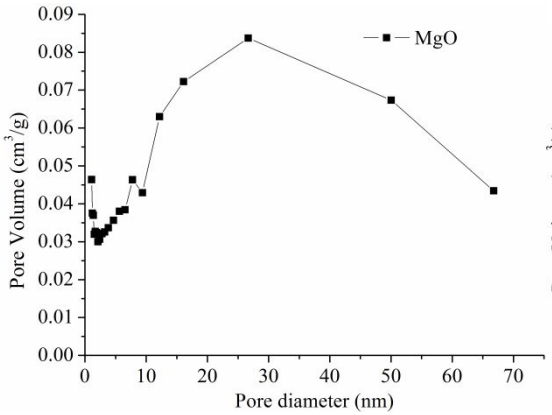
MgO
Pore Volume (cm3/g)
Pore diameter (nm)

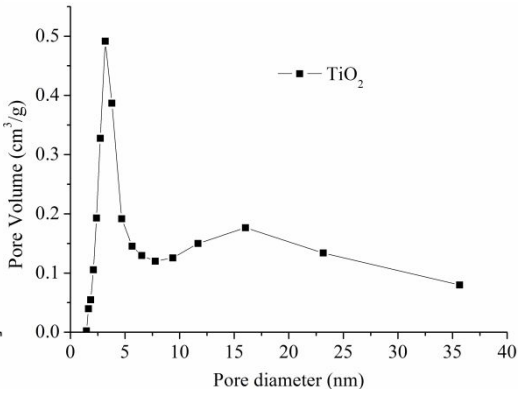
TiO2
Pore Volume (cm3/g)
Pore diameter (nm)

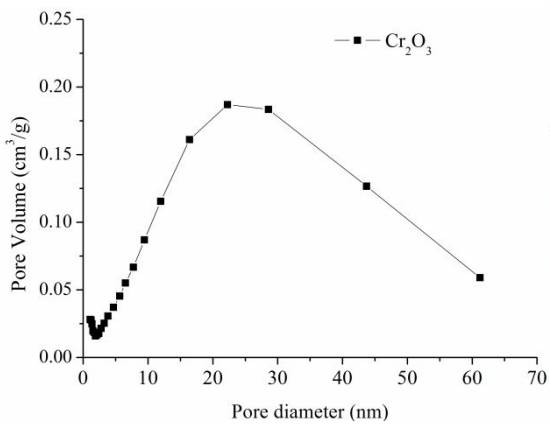
Cr2O3
Pore Volume (cm3/g)
Pore diameter (nm)

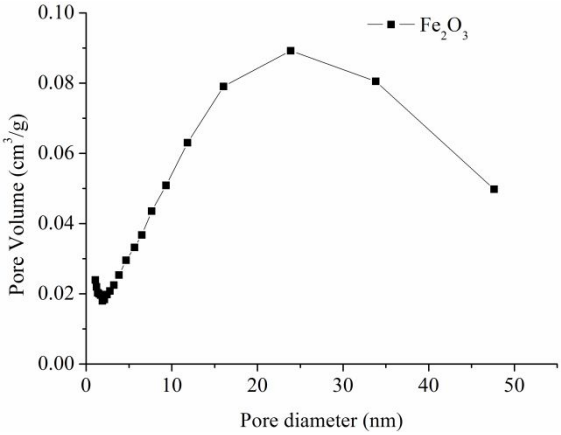
Fe2O3
Pore Volume (cm3/g)
Pore diameter (nm)

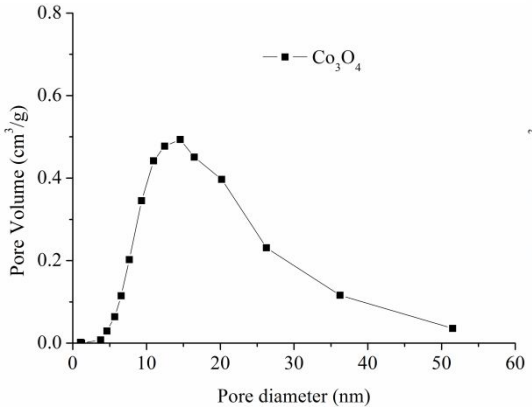
Co3O4
Pore Volume (cm3/g)
Pore diameter (nm)

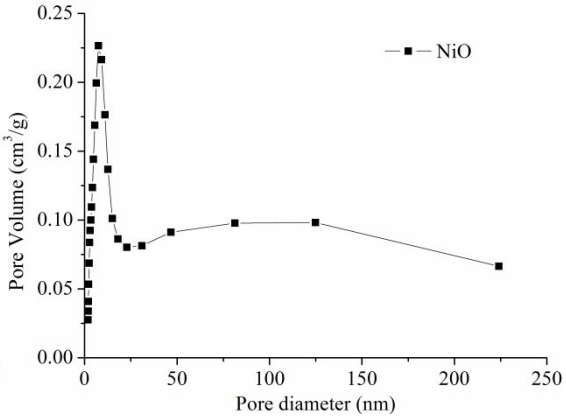
NiO
Pore Volume (cm3/g)
Pore diameter (nm)

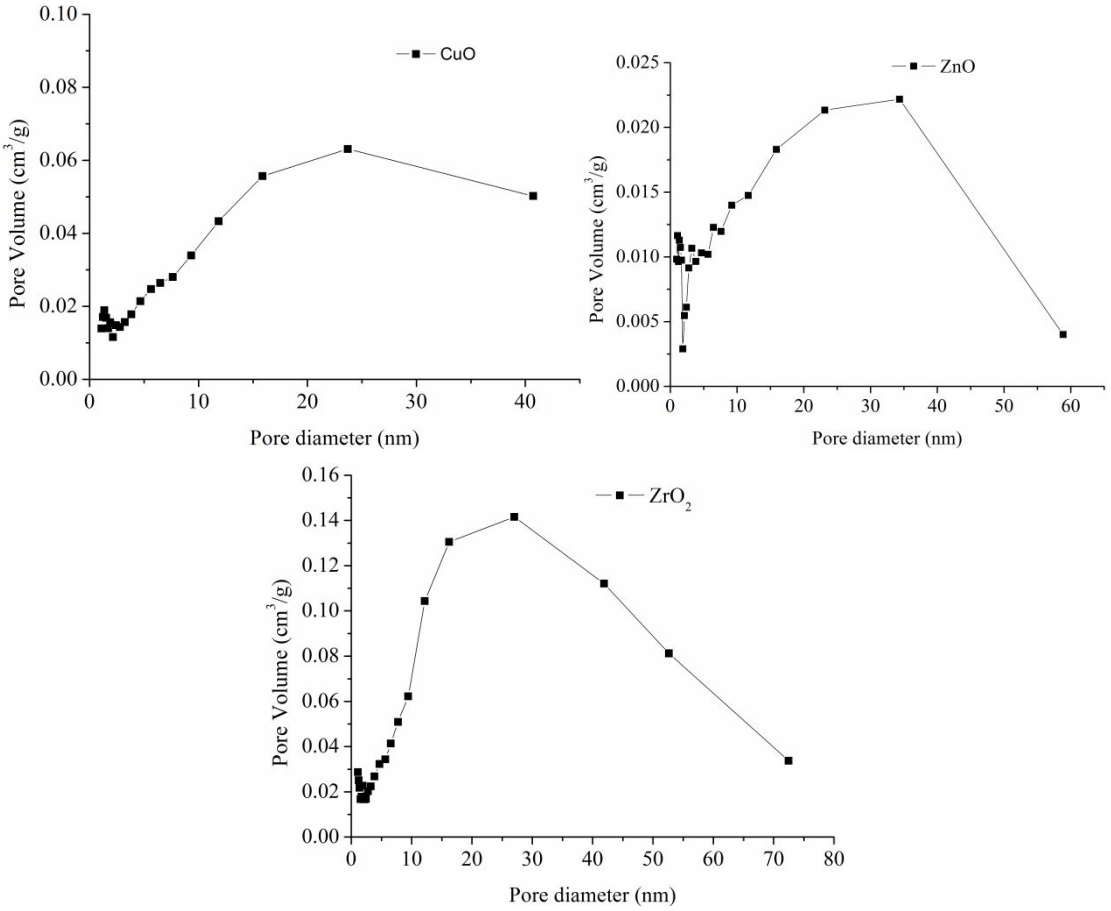


**Figure S1** Pore size distribution of different metal oxides nanoparticles.

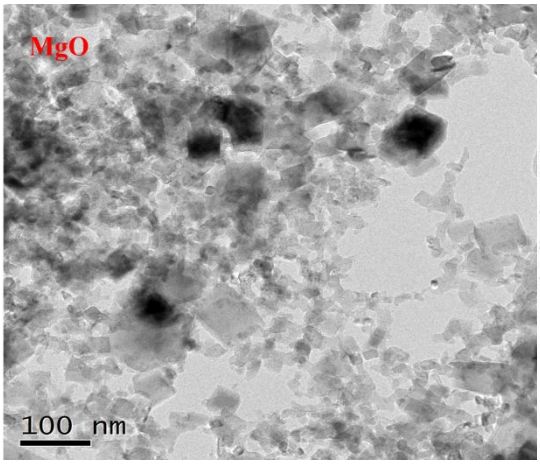
MgO
100 nm

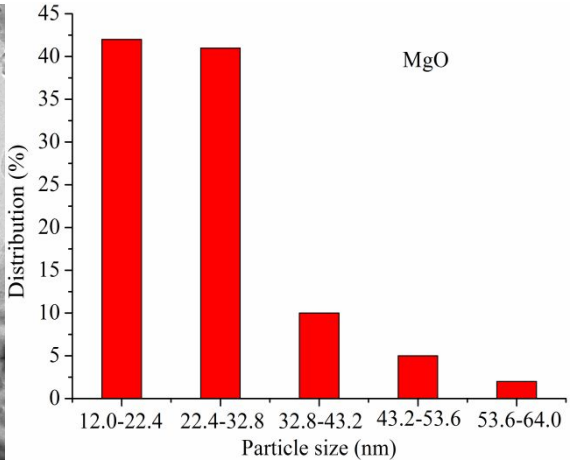
MgO
Distribution (%)
0
5
10
15
20
25
30
35
40
45
12.0-22.4
22.4-32.8
32.8-43.2
43.2-53.6
53.6-64.0
Particle size (nm)

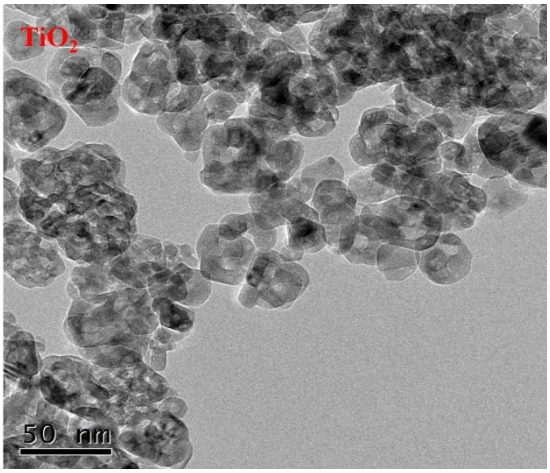
TiO2
50 nm

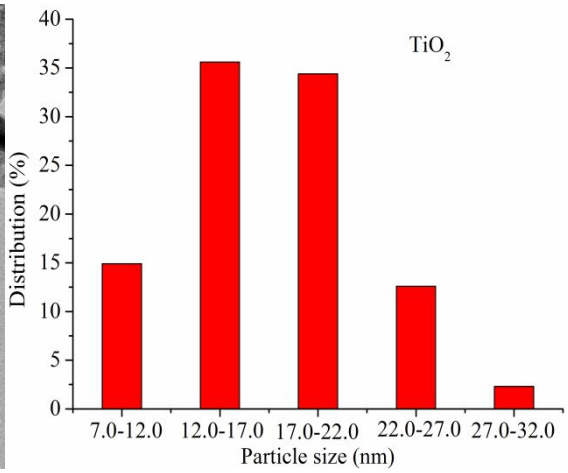
TiO2
Distribution (%)
0
5
10
15
20
25
30
35
40
7.0-12.0
12.0-17.0
17.0-22.0
22.0-27.0
27.0-32.0
Particle size (nm)

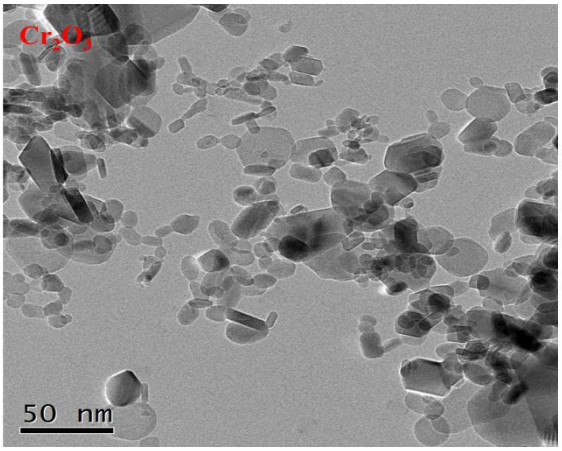
Cr2O3
50 nm

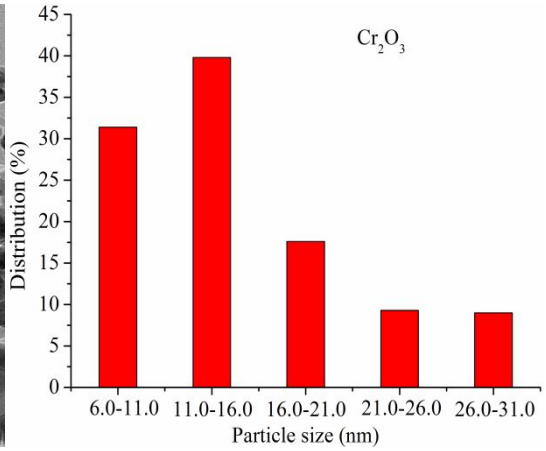
Cr2O3
Distribution (%)
0
5
10
15
20
25
30
35
40
45
6.0-11.0
11.0-16.0
16.0-21.0
21.0-26.0
26.0-31.0
Particle size (nm)

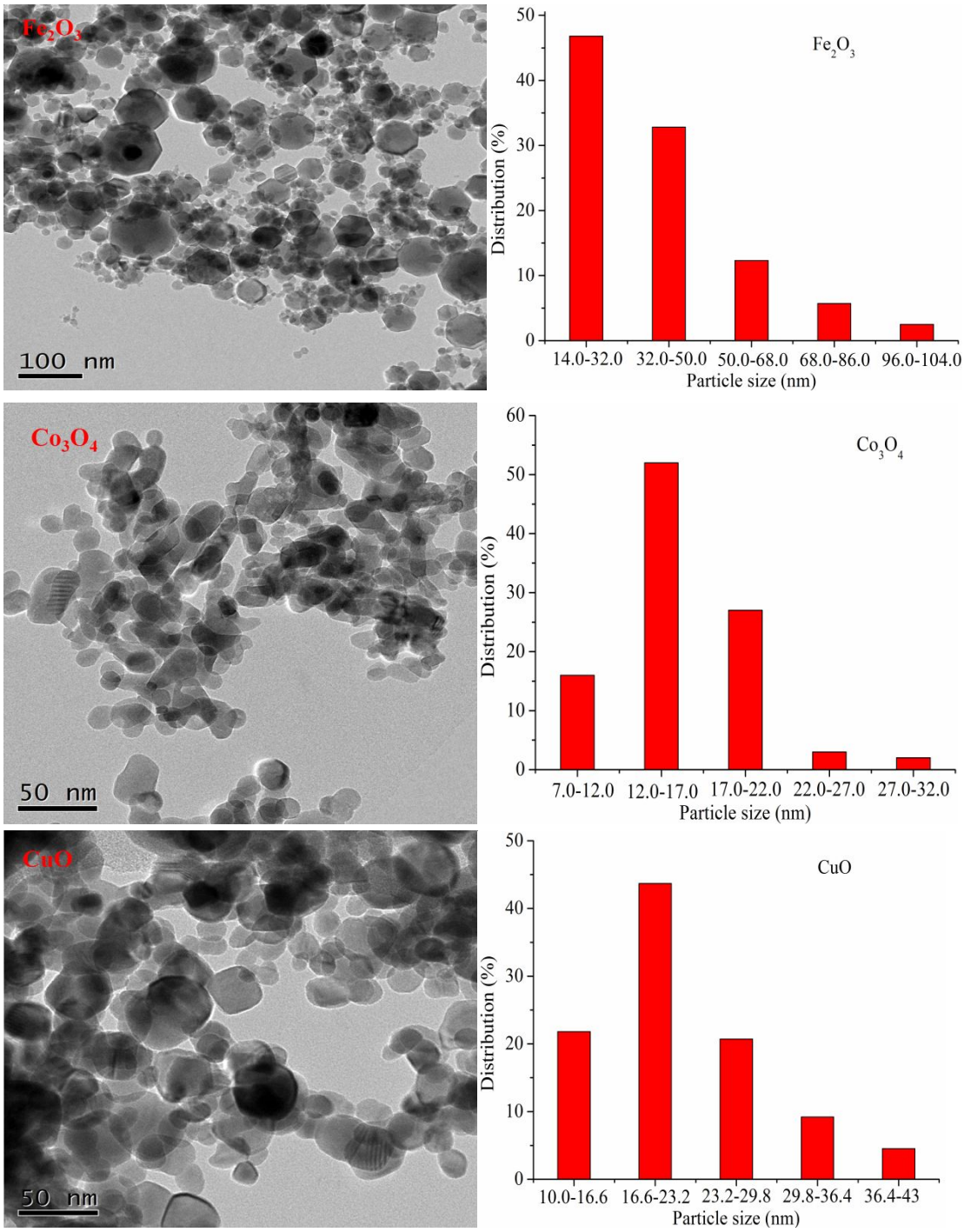
Fe2O3
100 nm
Fe2O3
Distribution (%)
0
10
20
30
40
50
14.0-32.0
32.0-50.0
50.0-68.0
68.0-86.0
96.0-104.0
Particle size (nm)
Co3O4
50 nm
Co3O4
Distribution (%)
0
10
20
30
40
50
60
7.0-12.0
12.0-17.0
17.0-22.0
22.0-27.0
27.0-32.0
Particle size (nm)
CuO
50 nm
CuO
Distribution (%)
0
10
20
30
40
50
10.0-16.6
16.6-23.2
23.2-29.8
29.8-36.4
36.4-43
Particle size (nm)

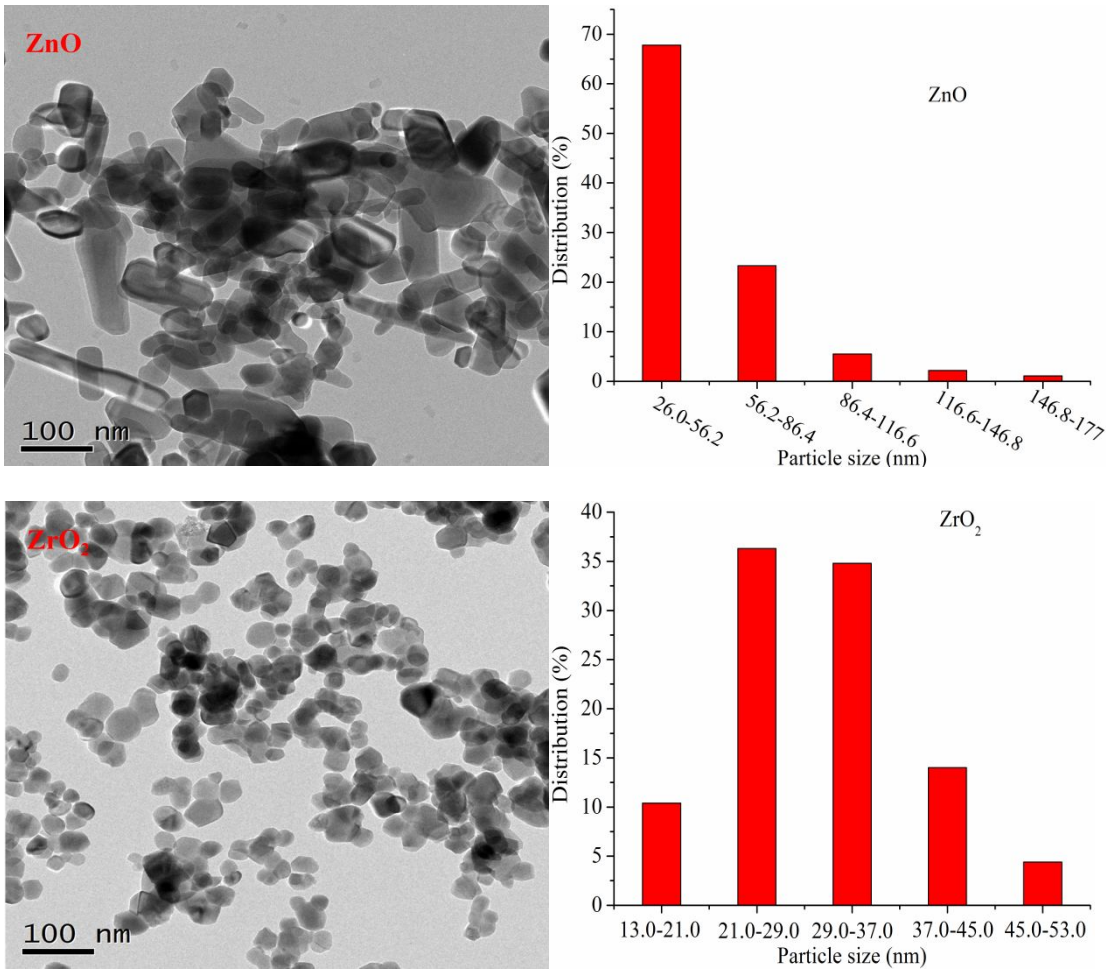


**Figure S2.** TEM images and particle size distributions of different metal oxide nanoparticles.

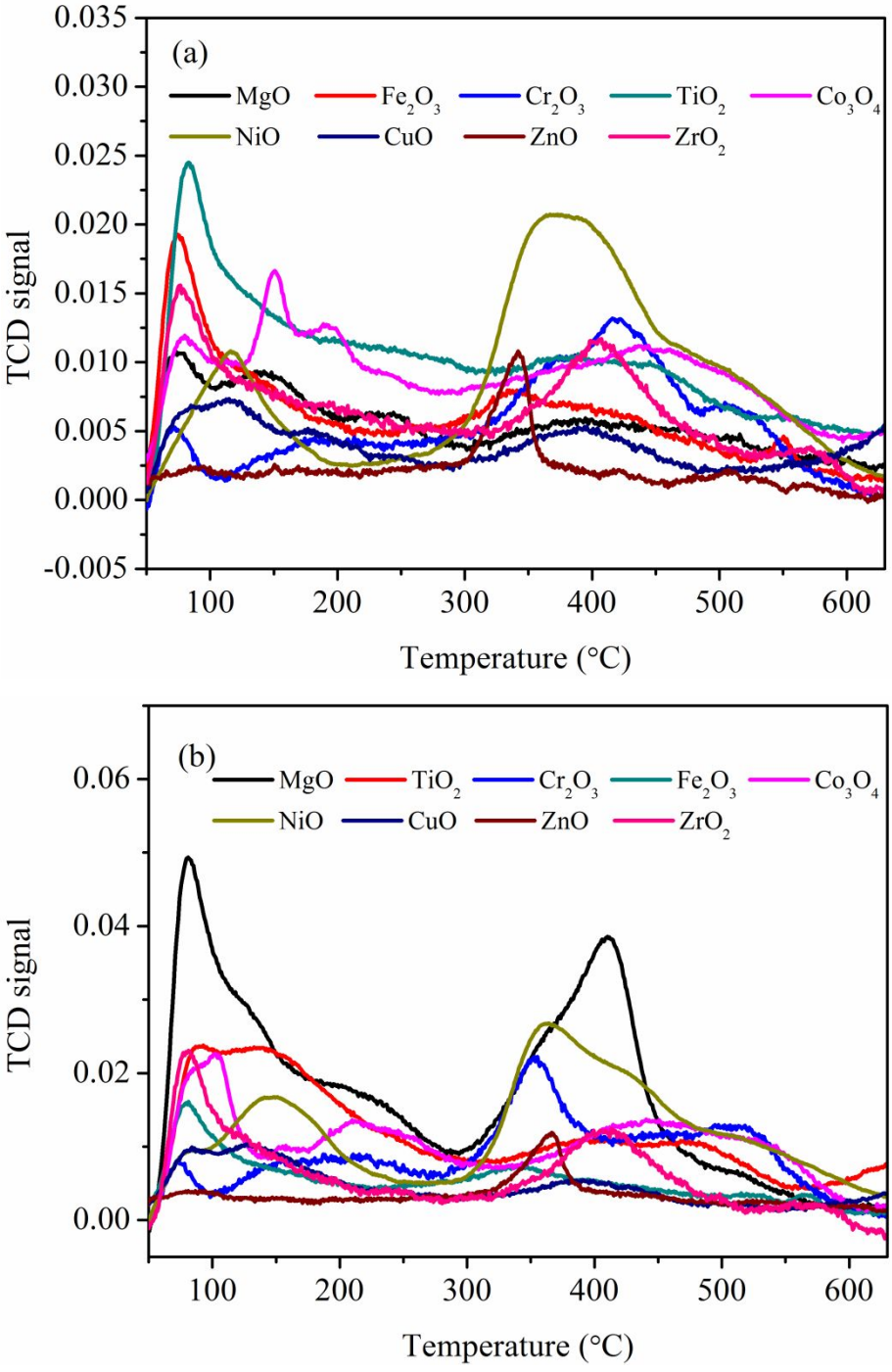


**Figure S3.** (a) $NH_3$-TPD and (b) $CO_2$-TPD profiles of catalysts.

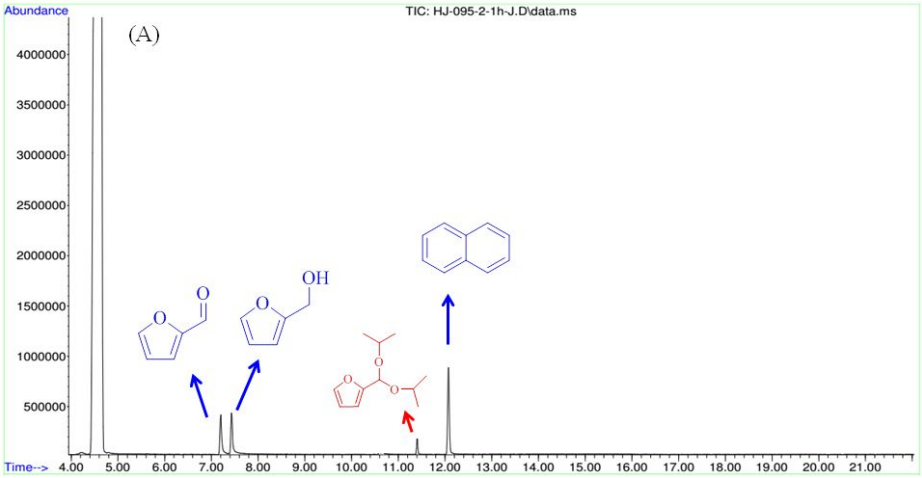
Abundance
TIC: HJ-095-2-1h-J.D\data.ms
(A)
4000000
3500000
3000000
2500000
2000000
1500000
1000000
500000
Time-->
4.00 5.00 6.00 7.00 8.00 9.00 10.00 11.00 12.00 13.00 14.00 15.00 16.00 17.00 18.00 19.00 20.00 21.00
O
OH
O
O
O

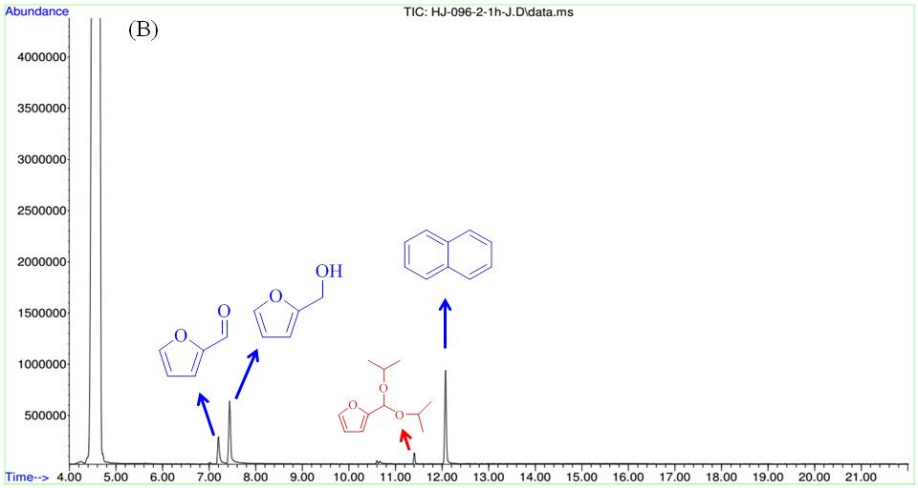
Abundance
TIC: HJ-096-2-1h-J.D\data.ms
(B)
4000000
3500000
3000000
2500000
2000000
1500000
1000000
500000
Time-->
4.00 5.00 6.00 7.00 8.00 9.00 10.00 11.00 12.00 13.00 14.00 15.00 16.00 17.00 18.00 19.00 20.00 21.00
O
OH
O
O
O

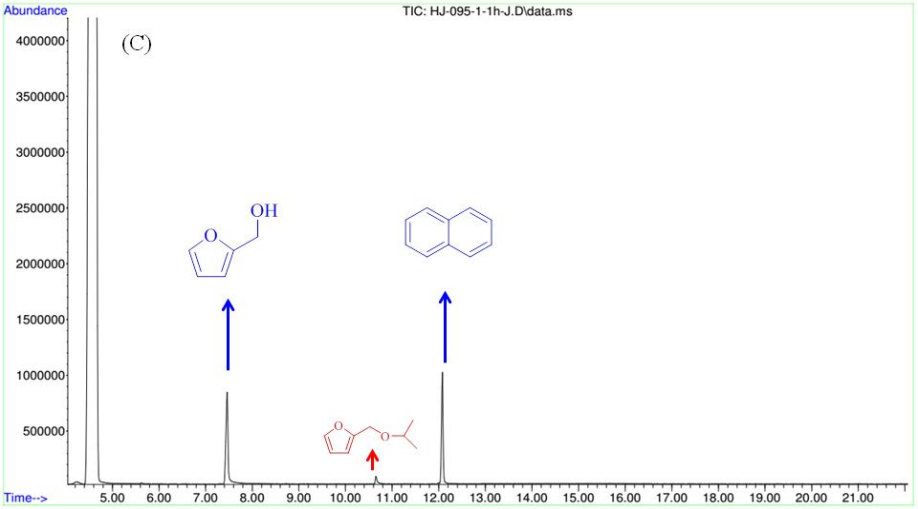
Abundance
TIC: HJ-095-1-1h-J.D\data.ms
(C)
4000000
3500000
3000000
2500000
2000000
1500000
1000000
500000
Time-->
5.00 6.00 7.00 8.00 9.00 10.00 11.00 12.00 13.00 14.00 15.00 16.00 17.00 18.00 19.00 20.00 21.00
OH
O
O

**Figure S4**. GC spectra with the main retention times (from GC-MS) of the reaction mixtures catalyzed by NiO catalyst illustrated in Table 3: (A) 130 °C, 1 h; (B) 150 °C, 1 h; (C) 170 °C, 1 h.

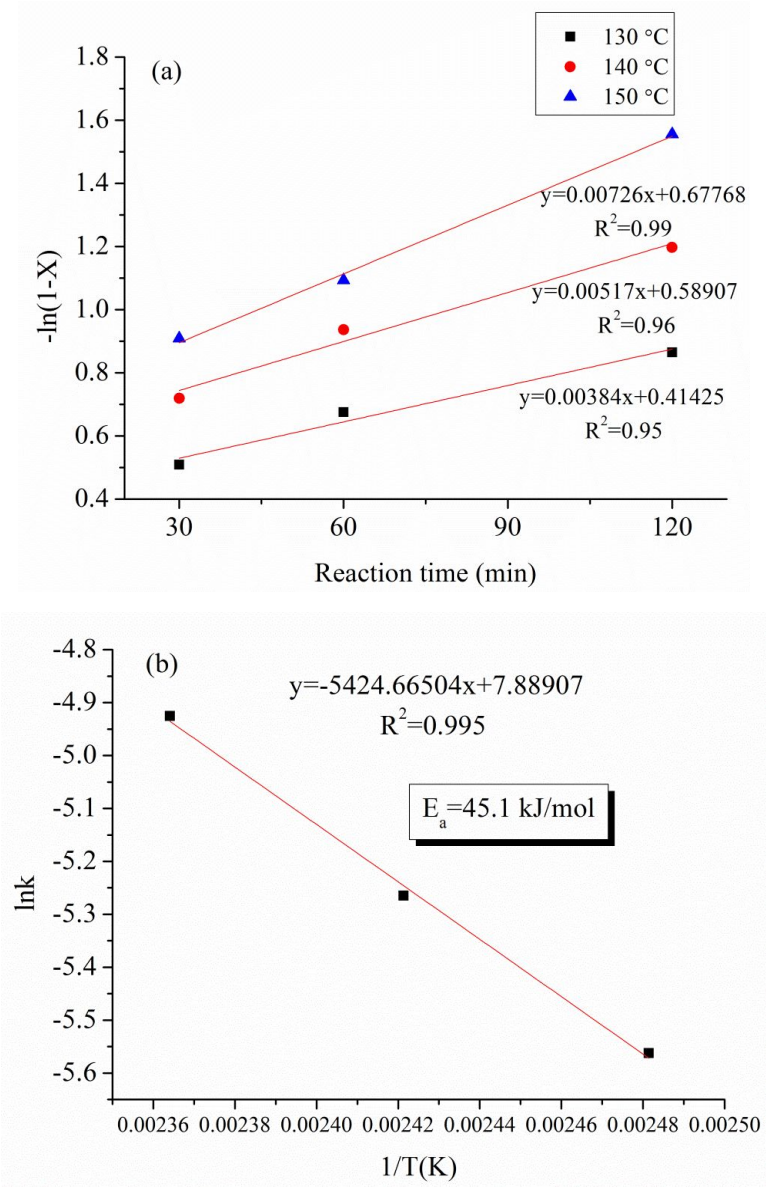


**Figure S5.** First-order kinetic fit for the CTH of FF to FAOL at (a) different temperature and (b) Arrhenius plot of conversion of FF to FAOL. Reaction conditions: FF (0.192 g, 2 mmol), NiO (0.08 g), 2-propanol (10.0 mL), 130-150 °C, 0.5-2 h.

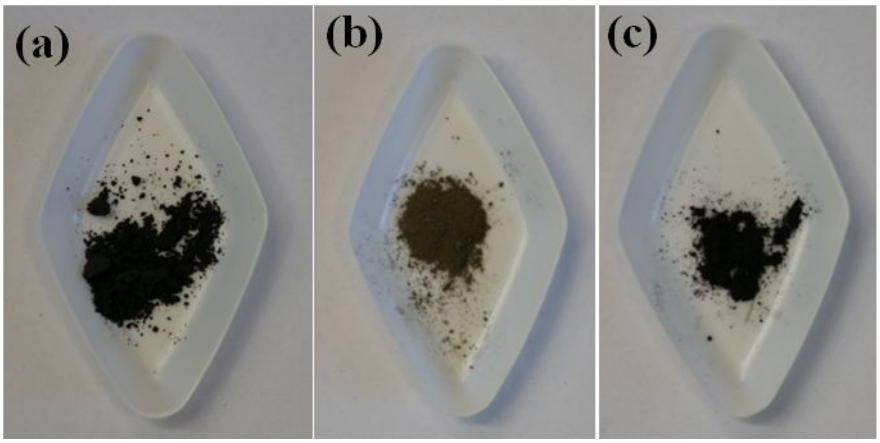


**Figure S6**. Pictures of (a) fresh, (b) used and (c) regenerated NiO catalyst.

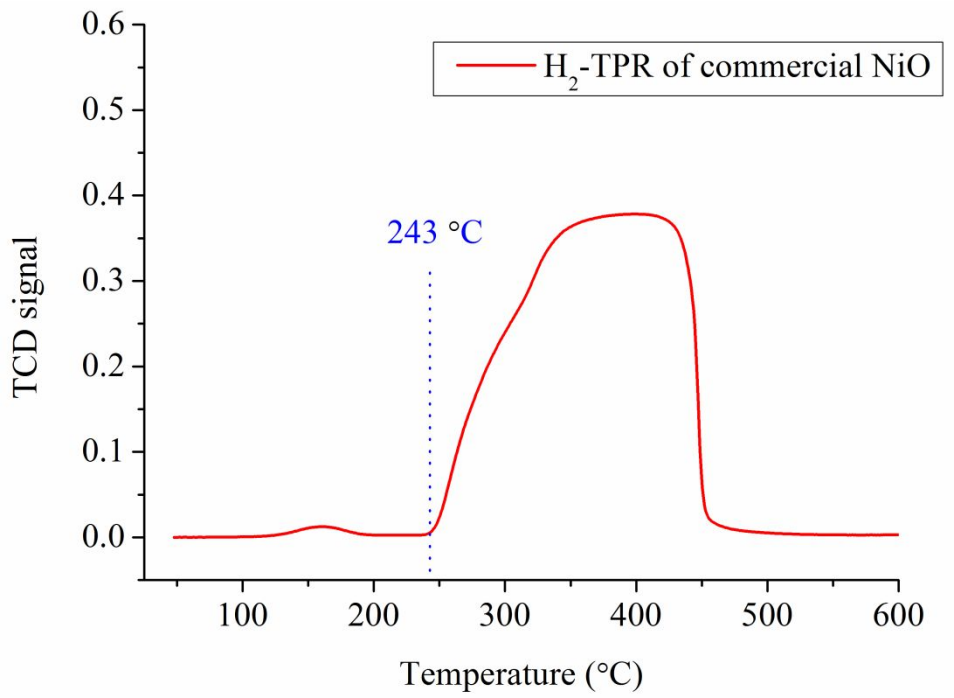


**Figure S7**. TPR profile of commercial NiO nanoparticles.

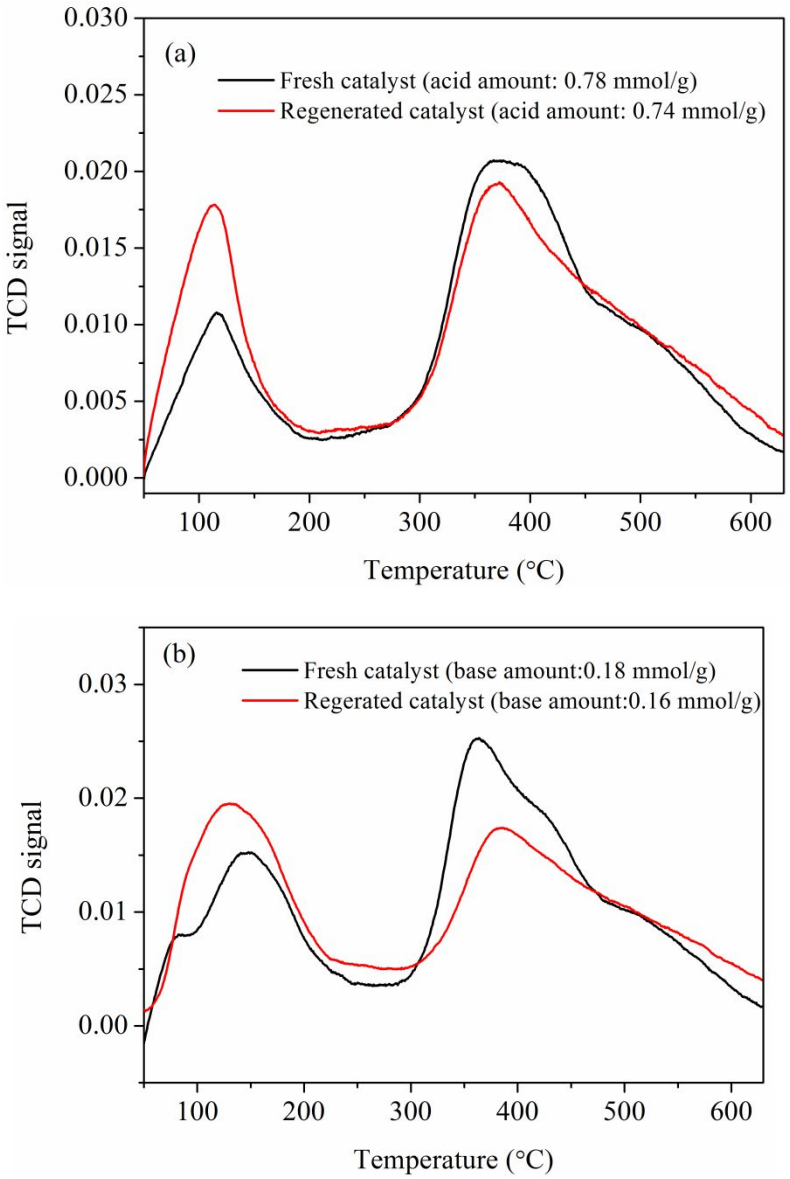


**Figure S8**. (a) $NH_3$-TPD and (b) $CO_2$-TPD profiles of fresh NiO catalyst and regenerated NiO catalyst after being recycled 5 times.

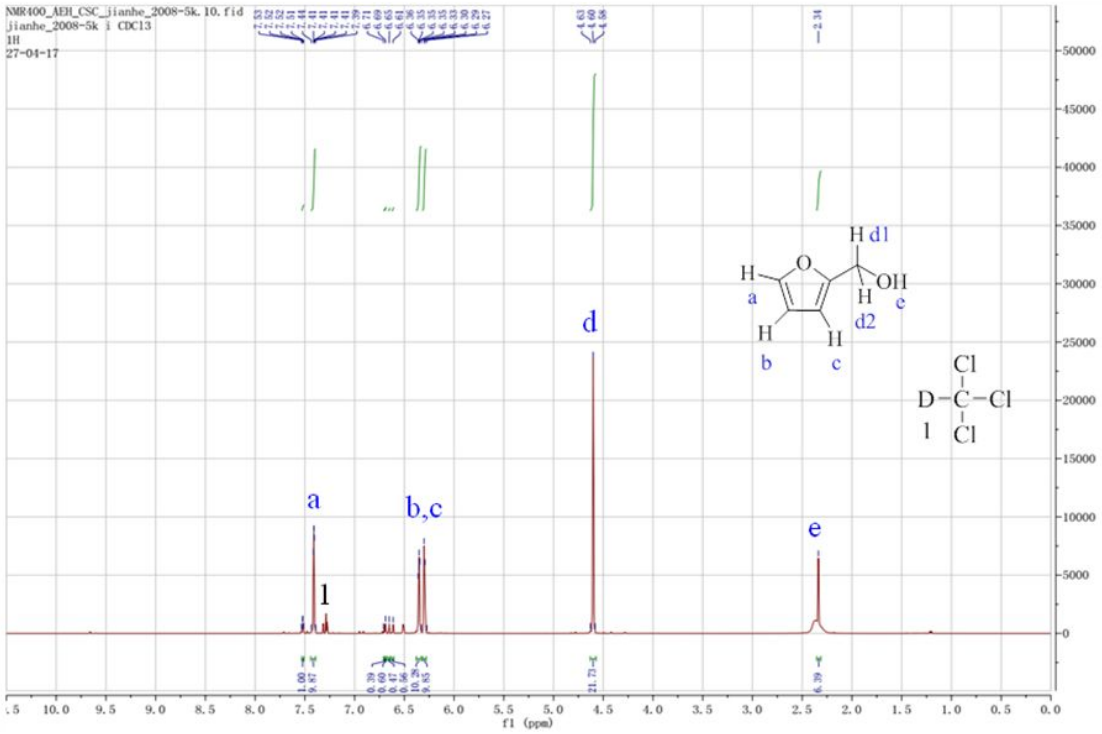


**Figure S9**. $^{1}$H NMR spectrum of the liquid product after CTH of FF and evaporation (the product was isolated by rotary evaporation at 70 °C under a reduced pressure of 50 mbar). Reaction conditions: Furfural (1.92 g), 2-propanol (25 mL), NiO catalyst (0.4 g), 170 °C, 5 h. Unmarked small peaks in the $^{1}$H-NMR spectrum are attributed to by-products.

**Table S1.** Particle size distributions of different metal oxides nanoparticles [a]

| Entry | Catalyst | Particle size (nm) | Content (%) |
|---|---|---|---|
| 1 | MgO | 12.0-32.8 | 83.0 |
| 2 | $TiO_2$ | 7.0-22.0 | 84.9 |
| 3 | $Cr_2O_3$ | 6.0-21.0 | 88.8 |
| 4 | $Fe_2O_3$ | 14.0-50.0 | 79.6 |
| 5 | $Co_3O_4$ | 7.0-22.0 | 95.0 |
| 6 | NiO | 9.0-18.0 | 84.8 |
| 7 | CuO | 10.0-29.8 | 86.2 |
| 8 | ZnO | 26.0-56.2 | 67.8 |
| 9 | $ZrO_2$ | 13.0-45.0 | 95.5 |

[a] Determined by TEM measurement.

**Table S2.** The acid and base strength distributions of different metal oxides nanoparticles

| Entry | Catalyst | Acid amount (mmol/g) | Acid strength distribution (%) | | Base amount (mmol/g) | Base strength distribution (%) | |
|---|---|---|---|---|---|---|---|
| | | | Weak (< 300 °C) | Moderate (300-500°C) | | Weak (< 300 °C) | Moderate (300-500°C) |
| 1 | MgO | 0.21 | 80.6 | 19.4 | 0.65 | 58.5 | 41.5 |
| 2 | $TiO_2$ | 0.59 | 89.1 | 10.9 | 0.15 | 79.4 | 20.6 |
| 3 | $Cr_2O_3$ | 0.49 | 5.1 | 94.9 | 0.13 | 5.6 | 94.4 |
| 4 | $Fe_2O_3$ | 0.29 | 63.4 | 36.6 | 0.07 | 64.4 | 35.6 |
| 5 | $Co_3O_4$ | 0.36 | 45.3 | 54.7 | 0.11 | 44.4 | 55.6 |
| 6 | NiO | 0.78 | 17.9 | 82.1 | 0.18 | 35.0 | 65.0 |
| 7 | CuO | 0.17 | 68.1 | 31.9 | 0.06 | 78.0 | 22.0 |
| 8 | ZnO | 0.08 | 10.0 | 90.0 | 0.05 | 6.7 | 93.3 |
| 9 | $ZrO_2$ | 0.39 | 54.9 | 45.1 | 0.12 | 64.2 | 35.8 |

**Table S3.** CTH of FF to FAOL over $ZrO_2$ catalysts [a]

| Entry | Catalyst | FF conv. (%) | FAOL yield (%) | FAOL Select. (%) |
|---|---|---|---|---|
| 1 | $ZrO_2$-300 [b] | 49.2 | 42.7 | 86.8 |
| 2 | $ZrO_2$-500 [b] | 29.4 | 23.5 | 80.0 |

[a] Reaction conditions: 2 mmol FF, 0.06 g catalyst, 10 mL 2-propanol, 150 °C, 1 h. [b] Zirconium dioxide was prepared by precipitation method and then calcined at 300 °C or 500 °C for 4 h, respectively.